

# Micro- and nanotechnology *via* reaction–diffusion

Bartosz A. Grzybowski,\* Kyle J. M. Bishop, Christopher J. Campbell, Marcin Fialkowski and Stoyan K. Smoukov

Received 2nd February 2005, Accepted 12th April 2005

First published as an Advance Article on the web 12th May 2005

DOI: 10.1039/b501769f

Reaction–diffusion (RD) processes are common throughout nature, which uses them routinely to build and control structures on length scales from molecular to macroscopic. At the same time, despite a long history of scientific research and a significant level of understanding of the basic aspects of RD, reaction–diffusion has remained an unrealized technological opportunity. This review suggests that RD systems can provide a versatile basis for applications in micro- and nanotechnology. Straightforward experimental methods are described that allow precise control of RD processes in complex microgeometries and enable fabrication of small-scale structures, devices, and functional systems. Uses of RD in sensory applications are also discussed.

## Introduction

Competition between reaction and diffusion can often lead to the emergence of intricate spatial and/or temporal structures,

which have been studied for more than a century<sup>1</sup> for their aesthetic appeal,<sup>2,3</sup> richness of dynamic behaviors,<sup>4,5</sup> theoretical challenges<sup>6,7</sup> and relevance to life.<sup>8,9</sup> The purpose of this review is to suggest that this list can and should be extended to



**Bartosz A. Grzybowski**

*Dreyfus New Faculty Award, and a co-founder of ProChimia and Micromorphix companies.*

*Bartosz A. Grzybowski graduated summa cum laude in Chemistry from Yale in 1995, obtained his PhD in Physical Chemistry from Harvard in 2000, and is now an assistant professor of Chemical and Biological Engineering at Northwestern University. His scientific interests include self-assembly in nonequilibrium/dynamic systems, non-equilibrium thermodynamics, complex chemical networks, nanostructured materials and molecular recognition. Dr Grzybowski is a recipient of the 2003 Camille and Henry*



**Kyle J. M. Bishop**

*approaches. Mr Bishop is an NSF Graduate Fellow.*

*Kyle J. M. Bishop received his undergraduate degree in Chemical Engineering from the University of Virginia in 2003. He is currently a PhD candidate working with Prof. Bartosz Grzybowski in the department of Chemical and Biological Engineering at Northwestern University. His research focuses spontaneous self-organization in non-equilibrium systems, both its fundamental understanding and its application to novel micro- and nano-engineering*



**Christopher J. Campbell**

*organization. Mr Campbell was an NSF/IGERT Fellow and has recently been awarded Northwestern Presidential Fellowship.*

*Christopher J. Campbell received his undergraduate degree in Chemical Engineering from the University of North Dakota in 2002. He is currently a PhD candidate working with Prof. Grzybowski in the Department of Chemical and Biological Engineering at Northwestern University. His specialization is in the theory and application of reaction–diffusion processes that lead to non-equilibrium self-*



**Marcin Fialkowski**

*science journals. In 2003–2004, Dr Fialkowski was a NATO Postdoctoral Fellow.*

*Marcin Fialkowski received his PhD degree in Theoretical Physics from the Jagiellonian University (Krakow, Poland) in 1997. He is currently working with Prof. Grzybowski in the Department of Chemical and Biological Engineering at Northwestern University. His specialization is in statistical and soft-matter physics and non-equilibrium/self-assembling systems. Dr Fialkowski has co-authored 30 refereed publications in leading physics, chemistry and materials*

**Table 1** Spatio-temporal patterns and structures created by RD processes

		Steady structures	Unsteady structures
Naturally occurring	Inanimate	Cave stalactites <sup>46</sup> Periodic precipitation <sup>47–52</sup> Limestone dendrites <sup>58</sup> Rock patterns <sup>47–51</sup>	Spiral galaxies <sup>20</sup> Forest fires <sup>19</sup>
	Animate	Bone formation <sup>181</sup> Limb development <sup>37–39</sup> Bacterial colonization <sup>41,42</sup> Skin patterns <sup>43–45</sup>  Pathological tissue structures <sup>105–111</sup>  Fingerprints <sup>44</sup>	Morphogenesis <sup>6,21</sup> Calcium oscillations and waves <sup>22,25–28</sup> Metabolic networks <sup>29</sup> Glycolytic oscillations <sup>182</sup> Microtubule formation <sup>31</sup> Neuronal synchronization <sup>34,183</sup> and dendrite formation <sup>184</sup> Cardiac arrhythmias <sup>35</sup> Atherosclerotic lesion formation <sup>36</sup> Slime mold aggregation <sup>40</sup>
Artificial	Science	Turing patterns <sup>6,14,96</sup> Periodic precipitation <sup>1,13,53–55</sup> Discharge filaments <sup>112–115</sup>	Periodic chemical oscillations <sup>15,68–70</sup> Chaotic chemical oscillations <sup>69,185–187</sup> Traveling waves <sup>15,69,71–74,80–82</sup> Externally controlled oscillators and waves <sup>75–79</sup>
	Technology	Wavelength selective diffraction gratings <sup>140</sup> Clogging of oil rigs <sup>188</sup> Non-binary photolithographic masks <sup>11</sup> Diffractive optical elements (Fresnel-like lenses) <sup>103,104</sup> Thermal (IR) cameras <sup>116–118</sup> Arrays of microlenses <sup>102,104</sup> Microfluidic channels <sup>141</sup> Static sensing <sup>171,172</sup> Microstructured foils <sup>159</sup> Surface and bulk microstructures <sup>170</sup>	Chemical waves on catalytic surfaces <sup>83–94</sup> Electrochemical oscillations <sup>83,95</sup> Antioxidant detection <sup>173,189</sup>

include reaction–diffusion (RD) as a possible basis of modern micro- and nanotechnologies.

We begin by briefly defining and classifying various types of RD systems. We then provide illustrative examples of how creatively and with what precision nature uses such systems to build and control structures on length scales from molecular to cosmic. As we shall see, this versatility is in sharp contradistinction to the current ability of science and technology to use RD in a controlled and/or purposeful manner. Nevertheless, we argue that with surprisingly simple experimental means, RD can become a new strategy for making small-scale structures, devices, and functional microsystems.

**Stoyan K. Smoukov**

*Stoyan K. Smoukov received his PhD degree in Physical Chemistry from Northwestern University in 2002. His emphasis in the Grzybowski lab is the creation of functionalized surface micropatterns, 3D surface nanotopographies, and new materials through programmable chemical reactions in microscopic environments.*

## Taxonomy of RD systems

The evolution of RD systems is governed by two essential components: (i) the reaction component describing local production or consumption of chemical species, and (ii) the diffusion component describing the diffusive transport of these species due to concentration gradients. Mathematically, these terms translate into a set of partial differential equations of the form:  $\partial C_i / \partial t = \nabla \cdot (D_i \nabla C_i) + R_i(\{C_j\}, r, t)$  where  $C_i$  is the concentration of species  $i$ ,  $D_i$  is its diffusion coefficient, and  $R$  is the reaction term. The inclusion of  $D_i$  in the gradient operator reflects the fact that diffusivities may vary spatially due to inhomogeneities in the medium, which may, themselves, be created by chemical reactions.<sup>10,11</sup> In the absence of spatial inhomogeneities, the dynamics of the system are governed purely by reaction kinetics and diffusion plays no role (e.g. in an ideal, continuously stirred tank reactor, CSTR<sup>12</sup>). In contrast, when no reactions are involved, RD equations simplify to the diffusion equation.

Patterns and structures created by RD processes can be classified (Table 1) as *steady* or *unsteady* as well as *static* or *dynamic*. Steady patterns are those which do not depend on time ( $\partial C_i(r, t) / \partial t = 0$ ). In a closed system, in which there is no flow of mass or energy, steady patterns are synonymous with equilibrium states and are necessarily static (e.g., Liesegang rings<sup>1,13</sup>). In contrast, steady, non-equilibrium patterns in open chemical systems (e.g., Turing patterns<sup>6,14</sup>) are *dynamic*<sup>3</sup> in the sense that they must be maintained far from equilibrium and are responsive to external stimuli. Other RD patterns are

time-dependent or unsteady ( $\partial C_i(r,t)/\partial t \neq 0$ ). In a closed system, periodic or chaotic structures may appear before eventually decaying to a static equilibrium state; in an open system, however, they may be maintained indefinitely by continuous supply of “food” and removal of “waste.”

We briefly note that although RD models are strictly valid to describe spatially distributed chemical and biochemical systems (e.g., the Belousov–Zhabotinsky (BZ) reaction,<sup>15</sup> calcium waves,<sup>16</sup> etc.), they have also been applied with considerable success to model non-molecular ensembles of interacting and diffusing objects: genes,<sup>17</sup> populations,<sup>18</sup> spreading forest fires<sup>19</sup> and even galaxies.<sup>20</sup> These and other examples will be discussed in detail in the next section.

## How nature uses RD (Fig. 1)

### (i) Animate systems

The idea that RD phenomena can be essential to the functioning of living organisms dates back to the seminal paper of Turing<sup>6</sup> who postulated their role in morphogenesis.<sup>21</sup> Since then, various cellular and organismal processes have been identified as relying on the competition between reaction and diffusion. On the transcriptional level, calcium oscillations are known to increase the efficiency and specificity of gene expression.<sup>22</sup> Calcium waves are also of prime importance in intracellular signaling.<sup>23,24</sup> Various types of calcium binding sites (e.g. calcium pumps like ATPase;<sup>25</sup> buffers like calbindin, calsequestrin and calretinin;<sup>26</sup> enzymes like phospholipases<sup>27</sup> and calmodulin<sup>28</sup>) interact with steep transient concentration gradients of calcium to create complex RD systems. Likewise, many aspects of cellular metabolism and energetics rely on reaction–diffusion: (i) glucose-induced oscillations and waves help coordinate the all-important process of glycolysis and other metabolic pathways; (ii) spatially arranged intracellular enzymatic networks, catalyzed by creatine kinase, adenylate kinase, carbonic anhydrase and glycolytic enzymes enable efficient high-energy phosphoryl transfer and signal communication between ATP-generating and ATP-consuming/sensing processes.<sup>29</sup> In order to overcome diffusional limitations, reactions in these networks are displaced from equilibrium, so that concentration wave fronts (“flux waves”) can travel rapidly over large distances.<sup>30</sup> Finally, cells use RD to build and dynamically maintain the microtubules, which are essential components of the cytoskeleton.<sup>31</sup>

Reaction–diffusion can span more than a single cell. Periodically firing neurons synchronize through RD-like coupling<sup>32,33</sup> which can extend over whole regions of the brain and propagate in the form of the so-called spreading depressions—that is, waves of potassium efflux followed by sodium influx.<sup>34</sup> Sometimes, the mode of propagation of intercellular RD patterns can distinguish between health and disease. For instance, if waves of electrochemical excitation in the heart’s myocardial tissue propagate as spirals,<sup>35</sup> they can lead to re-entrant cardiac arrhythmias such as ventricular tachycardia and fibrillation.<sup>36</sup>

In organismal development, RD is thought to mediate the directed growth of limbs. This process has been postulated<sup>37–39</sup> to involve transforming growth factor (TGF $\beta$ ) which stimulates production of fibronectin, and the formation of

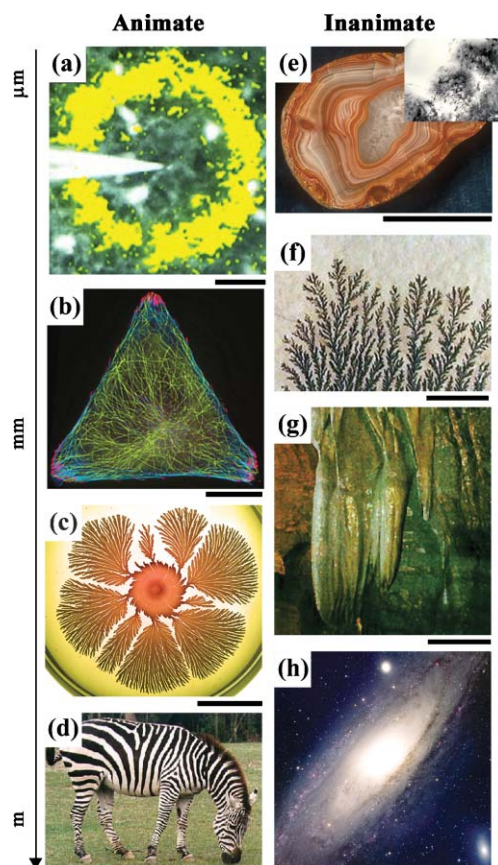


**Fig. 1** Examples of animate (a–d) and inanimate (e–h) reaction–diffusion systems on various length scales. (a) Calcium waves propagating in a retinal cell after mechanical stimulation (scale bar: 50  $\mu\text{m}$ ). (b) Fluorescently labeled microtubules in a cell confined to a 40  $\mu\text{m}$  triangle on a SAM-patterned surface of gold (staining scheme: green = microtubules, red = focal adhesions, blue = actin filaments; scale bar: 10  $\mu\text{m}$ ). (c) Bacterial colony growth (scale bar: 5 mm). (d) Turing patterns on a zebra. (e) Polished cross-section of a Brazilian agate (scale bar: 0.2  $\mu\text{m}$ ) with a transmission electron micrograph (inset) showing iris banding with a periodicity of 4  $\mu\text{m}$  (scale bar:  $\mu\text{m}$ ). (f) Dendritic formations on limestone (scale bar: 5 cm). (g) Cave stalactites (scale bar: 0.5 m). (h) Telescope image of the Andromeda galaxy. [Image credits: (a) E.A. Newman *et al.*<sup>23</sup> (b) Courtesy of K. Kandere-Grzybowska, Northwestern University. (c) Courtesy of E. Ben-Jacob, Tel Aviv University. (d) S. Kondo<sup>45</sup> (e) P. J. Heaney *et al.*<sup>52</sup> (f) Courtesy of Geoclassics.com. (g) Courtesy of M. Bishop, Niagara Cave, Minnesota. (h) Bill Schoening, Vanessa Harvey/REU program/NOAO/AURA/NSF]

fibronectin prepatterns (nodes) linking cells together into precartilaginous nodules. The nodules, in turn, actively recruit more cells from the surrounding area and inhibit the lateral formation of other foci of condensation and potential limb growth.

RD is sometimes used to coordinate collective development or defense/survival strategies of organism populations. For example, starved amoebic slime molds (e.g., *Dictyostelium discoideum*) emit spiral waves of cAMP that cause their aggregation into time-dependent spatial patterns.<sup>40</sup> Similarly, initially homogeneous bacterial cultures grown under conditions with insufficient nutrients form stationary,

non-equilibrium patterns to minimize the effects of environmental stress.<sup>41,42</sup>

Lastly, some biological RD processes give rise to patterns of amazing aesthetic appeal. Skin patterns in marine angelfish *Pomacanthus*<sup>43</sup> and in zebras, giraffes and tigers<sup>44,45</sup> are but a few examples.

## (ii) Inanimate systems (Fig. 1)

Reaction–diffusion is also behind many intricate creations composed of inorganic matter. Cave stalactites owe their shapes to RD processes<sup>46</sup> involving (i) hydrodynamics of a thin layer of water carrying  $\text{Ca}^{2+}$  and  $\text{H}^+$  ions and flowing down the stalactite, (ii) calcium carbonate reactions, and (iii) diffusive transport of carbon dioxide. Formation of a stalactite is a consequence of the locally varying thickness of the fluid layer controlling the transport of  $\text{CO}_2$  and the precipitation rate of  $\text{CaCO}_3$ .

Many natural minerals possess textures exhibiting compositional zoning (examples include plagioclase, garnet, augite, or Zebra Spa rock)<sup>47–51</sup> with alternating layers composed of different types of precipitates. An interesting example of two-mineral deposition is the alternation of defect-rich chalcedony and defect-poor quartz observed in iris agates.<sup>52</sup> The striking similarity to Liesegang rings<sup>13,53–55</sup> created in “artificial” RD systems, suggests that banding of mineral textures is governed by the Ostwald–Liesegang mechanism<sup>56</sup> or two-salt Liesegang mechanism.<sup>57</sup>

RD-driven dendritic structures appear on surfaces of limestone.<sup>58</sup> These dendrites are deposits of hydrous iron or manganese oxides formed when supersaturated solutions of iron or manganese diffuse through the limestone and precipitate at the surface on exposure to air. The structure of these mineral dendrites can be successfully described in terms of simple red-ox RD equations.<sup>59</sup> At this point a cautionary note regarding RD and dendritic growth is due. The example of limestone is probably the *only* one underlined by reaction–diffusion proper. Other dendritic systems, though often incorrectly classified and described as RD, are in fact results of simple diffusion-limited aggregation (DLA) processes.<sup>60–62</sup> The difference between RD and DLA is that in the latter, the growth equations are written in terms of only a single diffusing field (*e.g.* electric field in the case of electrochemical deposition,<sup>63</sup> temperature in dendritic growth,<sup>64,65</sup> and pressure field in viscous fingering<sup>66,67</sup>), and the reaction terms are missing. In contrast, RD processes must involve at least two different diffusing fields interacting through chemical reactions, or, in the case of a single-field description, autocatalytic terms.

RD makes not only small, but also very large structures. Recent work in astrophysics suggests that formation of spiral disks in isolated galaxies is an RD process,<sup>20</sup> and that the galactic disk can be treated as a self-regulated, non-equilibrium system of autocatalytic reactions, in which spiral stellar structures form and persist because of catalysis and inhibition.

## RD in science and technology (Fig. 2)

While nature uses reaction–diffusion in sophisticated functional ways, scientists have focused on model systems that

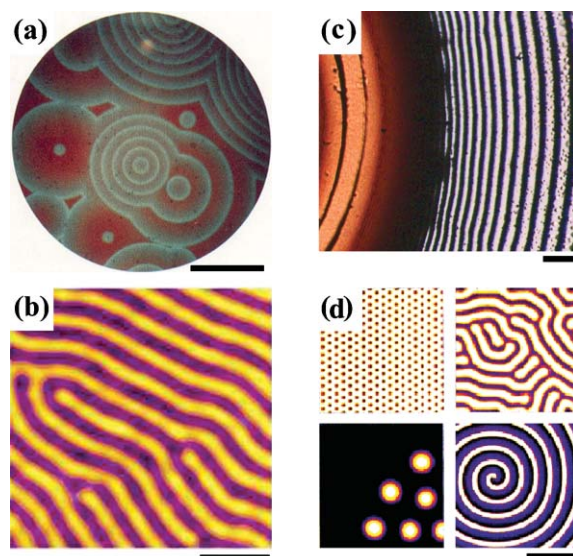


**Fig. 2** Man-made reaction–diffusion systems. (a) Traveling waves in the Belousov–Zhabotinsky chemical system (scale bar: 30 mm). (b) Turing pattern formed by CIMA reaction (scale bar: 5 mm). (c) Periodically-precipitated Liesegang rings of silver dichromate in a layer of gelatin (scale bar: 400  $\mu\text{m}$ ). (d) Patterns formed by discharge filaments (scale bar: 2 mm) [Image credits: (a) Courtesy of I. Epstein, Brandeis University. (b) Courtesy of J. Boissonade, CRPP Bordeaux. (c) Courtesy of A. Bitner, Northwestern University. (d) Courtesy of H.G. Purwins, University of Münster.]

capture the essential characteristics of RD processes. There are four major classes of such systems:

**(i) Chemical oscillators**, which have evolved from the status of a scientific curiosity<sup>68</sup> to a major branch of modern non-linear science. The classic Belousov–Zhabotinsky (BZ) reaction is an “ancestor” of whole families<sup>15,69</sup> of chemical systems exhibiting either bulk oscillations (*e.g.*, Briggs–Rauscher iodine clock<sup>70</sup>) or both oscillations and chemical wave propagation.<sup>71–74</sup> The study of these systems has laid a solid foundation for the theoretical description of RD processes and facilitated the understanding of many natural phenomena described in the preceding section. Recently, with an increasing level of experimental control, significant progress has been made in controlling chemical oscillators by external means (*e.g.*, by light,<sup>75,76</sup> electric impulses,<sup>77</sup> or physical/electrochemical introduction of metal ions<sup>78,79</sup>) and in extending them into three-dimensions.<sup>80–82</sup>

Of particular technological relevance are chemical waves propagating on catalytic surfaces,<sup>83</sup> *e.g.* during oxidation of CO on platinum,<sup>84–86</sup> palladium,<sup>87</sup> rhodium<sup>88</sup> and iridium,<sup>89</sup> as well as NO oxidation over platinum<sup>90–92</sup> and rhodium.<sup>93</sup> Interestingly, such waves can sometimes physically pattern the substrate on which they move (*e.g.*, knotted rope-web and honeycomb surface patterns were observed in zeolites<sup>94</sup>). Finally, electrochemical oscillations on metal electrodes are studied for their relevance to the issues of corrosion<sup>95</sup> and catalysis.<sup>83</sup>

**(ii) Turing patterns** are stationary patterns of chemical concentrations that emerge as the result of a symmetry-breaking instability in an RD system far from equilibrium.<sup>6,14,96</sup> Formation of these dissipative structures requires: (i) an

“activator” A that can catalyze its own production, (ii) an “inhibitor” B that poisons the autocatalytic process, and (iii) a difference in diffusivities such that  $D_A \ll D_B$ . Under such conditions, an initially homogeneous mixture may give way to stationary patterns, in which regions rich in A are bounded by the fast-diffusing inhibitor B. Because these patterns only occur far from equilibrium, they need a continuous supply/removal of chemicals to survive and appear only fleetingly in a closed system. Several RD systems exhibiting the Turing instability have been successfully developed<sup>97</sup> to reproduce the formation of zebra stripes, leopard spots, and labyrinthine patterns of sea urchin shells. The Turing mechanism is also responsible for pattern formation in a number of chemical RD systems such as CIMA (chlorite–iodide malonic acid) and CDIMA reactions (chlorine dioxide–iodine malonic acid)<sup>14,96,98,99</sup> as well as model chemical systems such as the Brusselator<sup>7</sup> and the Oregonator.<sup>100,101</sup>

(iii) **Periodic precipitation (PP) structures** emerge when inorganic salts diffusing through a gel form mobile colloidal precipitates that can subsequently aggregate into an immobile phase. Since their discovery in 1896 by Liesegang,<sup>1</sup> these structures have been miniaturized from macroscopic to sub-millimeter dimensions, and their applications in optics have recently been suggested.<sup>102–104</sup> PP patterns are also interesting in the context of human health, as periodic precipitation zones have been identified in several types of pathological tissues.<sup>105–111</sup>

(iv) **Discharge filaments** between parallel electrodes<sup>112</sup> are of less generality than chemical RD systems. Over the last decade, however, continuing iteration of modelling and experiments has led to the discovery of many types of patterns in these systems; examples include: Voronoi tessellations,<sup>113</sup> concentric rings,<sup>114</sup> and rotating hexagonal arrays.<sup>115</sup> Since discharge filaments are very sensitive to the temperature of the electrode surfaces, these systems have been considered as working elements of sensitive, high-speed thermal (IR) cameras.<sup>116–118</sup>

Although several directions can be envisioned for further development of reaction–diffusion processes, there are no technological applications of these systems yet. On the contrary, RD phenomena often cause untoward complications. For example, oxidation waves on catalytic converters in automobiles and in catalytic packed bed reactors introduce highly nonlinear, and potentially even chaotic<sup>86</sup>, temperature and concentration variations that are challenging to design around, problematic to control, and can drastically affect automobile emissions.<sup>119</sup> In catalytic packed bed reactors, nonlinearities introduce hot zones,<sup>120</sup> concentration waves,<sup>121</sup> and unsteady temperature profiles<sup>122</sup> that can prevent the system from attaining optimal performance. These phenomena have significant impacts for industry (economic), as well as for the environment (societal).

## RD—from here to nanotechnology

The major obstacle to successful implementation of RD phenomena in modern technologies has been the lack of control over their progress and the geometries in which they occur. For example, regular microstructures emerging in salt-doped gels by periodic precipitation have been postulated as

potentially useful in optics (*e.g.*, as diffraction gratings) but so far could be propagated only from simplest macroscopic geometries such as lines or circles. In addition, the initiating chemicals were delivered into gels from solution, causing strong hydrodynamic flows, suppressing the formation of PP patterns and thus decreasing their spatial resolution.

Notwithstanding, should it be possible to control the transport of reacting chemicals at small scales precisely, RD could become a basis of new and in many ways elegant approaches to the synthesis of micro- and nanostructures. There are several arguments in favor of this view:

(i) RD could generate structures with dimensions significantly *smaller* than those characterizing the initial distribution of reagents. Liesegang rings can be much thinner than the droplet of the outer electrolyte from which they originate, arms of growing dendrites are minuscule in comparison to the dimensions of the whole structure, and the characteristic length of the pattern created through the Turing mechanism is usually much smaller than the dimensions of the system containing the reactants.

(ii) The emergence of small structures could be *programmed* by the initial conditions of an RD process—that is, by the initial concentrations of the chemicals and by their spatial locations. In particular, several chemical reactions could be started simultaneously, each performing an independent task to enable parallel fabrication.

(iii) RD could produce patterns encoding spatial gradients. This capability would be especially important in the context of surface micropatterning; methods currently in use (photolithography,<sup>123,124</sup> printing<sup>125,126</sup>) modify substrates only at the locations to which a modifying agent, whether chemical<sup>127,128</sup> or radiation<sup>129,130</sup>, is delivered. In contrast, RD could evolve chemicals from their initial (patterned) locations in the plane of the substrate and deposit them onto this substrate at quantities proportional to their local concentrations. Gradient-patterned surfaces would be of great interest in cell motility assays,<sup>131,132</sup> biomaterials<sup>133,134</sup> and optics.<sup>135,136</sup>

(iv) RD processes could be coupled to chemical reactions involving the medium in which they occur. In this way, RD structures could be translated into, for example, localized mechanical properties or surface topographies of the initially uniform material supporting reaction–diffusion processes.

Moreover, the possibility of coupling RD to other processes occurring in the environment could have implications for the uses of reaction–diffusion in sensing/detection applications. The inherent nonlinearity of RD equations implies their high sensitivity to parameter changes and suggests that they could amplify small signals, influencing RD dynamics. Of particular promise here would be systems capable of translating molecular or nanoscale events into macroscopic readout patterns. One such recent example is the monitoring of the progress of the  $2\text{H}_2\text{O} + \text{O} \rightarrow 3 \text{OH} + \text{H}$  surface reaction by the velocity of propagation of the corresponding 20 nm wide reaction front.<sup>137,138</sup>

At this point, the reader might ask whether these enticing perspectives are in any way realistic, especially given that RD phenomena have been studied vigorously for more than a century but without much success in terms of technological relevance. In the following, however, we will argue that RD

can be brought under experimental control at small scales by surprisingly simple experimental means, and that it can be made to perform useful tasks in micro- and nanotechnology.

### Micropatterning reaction–diffusion by WETS

Over the past two years, our group has developed<sup>7,10,13,136–141</sup> an experimental technique that allows initiation and precise control of reaction–diffusion processes in complex microgeometries. In its simplest variation, our method—called ‘wet stamping’ or ‘WETS’—uses micropatterned hydrogel (usually, agarose) stamps to deliver a solution of one or more reactants into films of dry gels (typically, gelatin) doped with chemical(s) that react with those delivered from the stamp (Fig. 3a).

The difference in hydration of the two gels ensures directional mass transport.<sup>139</sup> Because the concentration of solute molecules is higher in the dry film than in the stamp, a gradient of osmotic pressure exists between the phases. When the stamp is placed onto the film, water and reactants migrate from the tops of its microfeatures into the dry gel without any backflows. The transport of water itself has two components: (i) rapid ( $\sim 1.5 \mu\text{m s}^{-1}$ ) capillary wetting of the surface and (ii) slow diffusive transport into gelatin’s bulk ( $D_w \sim 10^{-7} \text{cm}^2 \text{s}^{-1}$ ), during which water dissolves the solute and swells the gel’s pores; this transport ceases when the gradient of osmotic pressure is balanced by the elastic potential energy of the swollen gel.

When the reactants from the stamp enter the gelatin, they react with the solute molecules contained therein. Because the reaction(s) consume delivered reactants, their local concentrations have to be diffusively resupplied from the stamp. As a result, the reaction front travels slower (typical diffusion constant in the plane of the surface,  $D_s \sim 10^{-5} \text{cm}^2 \text{s}^{-1}$ ) than water swelling the gelatin. In other words, reactants entering the gel diffuse and react in a thin, already swollen layer of gel near the surface. The thickness of this layer,  $d_w$ , can be estimated from the relation  $d_w \sim \sqrt{D_w/D_s} L_s$ , where  $L_s$  is a characteristic distance the reaction front travels (typically, from tens to hundreds of micrometres, depending on a particular chemistry); and with the typical values of the diffusion coefficients measured for gelatin,  $d_w$  is of the order of several to tens of micrometres.

#### (i) Color micro- and nanopatterning (Fig. 3)

The first class of RD applications based on WETS uses ionic salts to produce static, colored micro- and nanopatterns.<sup>11</sup> In these systems, gelatin is doped with potassium hexacyanoferrate,  $\text{K}_4\text{Fe}(\text{CN})_6$  and the salts delivered from a stamp are chosen in such a way that their cations react with  $\text{K}_4\text{Fe}(\text{CN})_6$  to give deeply colored precipitates. For example,  $\text{FeCl}_3$  gives a dark-blue precipitate (Prussian Blue);  $\text{CoCl}_2$ , turquoise and  $\text{CuCl}_2$ , brown.

As the cations constantly delivered from the stamp migrate into gelatin, they precipitate all  $\text{K}_4\text{Fe}(\text{CN})_6$  they encounter. The unreacted potassium hexacyanoferrate experiences a sharp concentration gradient at the reaction front, and diffuses in its direction. In the case of two reaction fronts counter-propagating from nearby features of the stamp, potassium hexacyanoferrate between them diffuses outwards—that is,

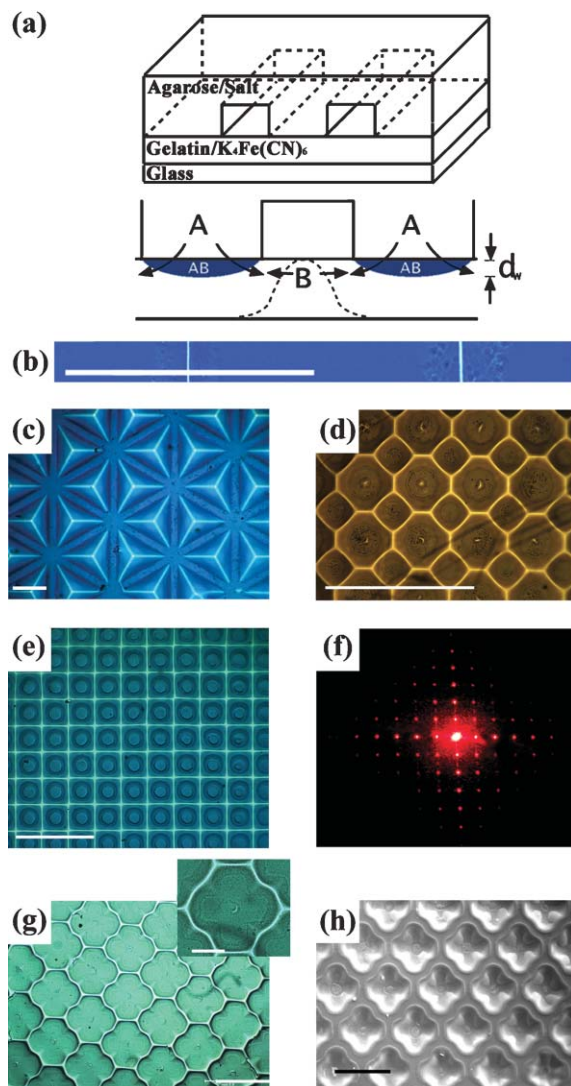


**Fig. 3** One-color RD micropatterning. The experimental setup in (a) shows an agarose stamp micropatterned in bas-relief, soaked in a salt solution (e.g.  $\text{FeCl}_3$ ,  $\text{CoCl}_2$ , or  $\text{CuCl}_2$ ) and applied onto a thin film of dry gelatin doped with  $\text{K}_4\text{Fe}(\text{CN})_6$ . Typically, the stamp’s features are 25–250  $\mu\text{m}$  wide and are spaced by 50–250  $\mu\text{m}$ . The scheme below illustrates the reaction–diffusion process inside the patterned gel, in which the salt solution from the stamp (A) wets a thin layer (depth,  $d_w \sim 10 \mu\text{m}$ ) of dry gelatin and reacts therein with the salt (B) to form an immobile precipitate (AB). Arrows indicate the directions of diffusion of A and B ions. (b) Nanoscale resolution of lines from stamping 1.0 M  $\text{FeCl}_3$  on a gel doped with 1% w/w  $\text{K}_4\text{Fe}(\text{CN})_6$ . The line width is 300 nm, and the scale bar is 50  $\mu\text{m}$ . The pictures in (c) and (d) are Voronoi tessellations of wet-stamped patterns: (c) a hexagonal network of side 300  $\mu\text{m}$  stamped from 1.0 M  $\text{FeCl}_3$ ; (d) an array of circles of two sizes (50  $\mu\text{m}$  and 100  $\mu\text{m}$ ) stamped from 1.0 M  $\text{CuCl}_2$ . (The scale bars are 250  $\mu\text{m}$ ). Applications of one-color RD micropatterning are illustrated in (e)–(h). In (e), a stamp of 50  $\mu\text{m}$  circles spaced by 50  $\mu\text{m}$  yielded a square array of  $\sim 4 \mu\text{m}$  wide clear lines that was subsequently used to produce the diffraction pattern shown in (f) ( $\lambda = 632 \text{ nm}$ ). An array of crosses in (g) stamped from 0.75 M  $\text{CoCl}_2$  created concentration gradients of the precipitate. The patterned substrate was used as a gradient photolithographic mask to produce a three-dimensional pattern in photoresist (h) (UV exposure on silicon wafer spin-coated with 50  $\mu\text{m}$  of SU-8 50 photoresist). The scale bars for (e)–(h) are 300  $\mu\text{m}$ .

towards the incoming fronts (Fig. 3a). This outflow continues until, ultimately, there is no more potassium hexacyanoferrate left near the center line between the features. Although the cations continue to diffuse into this region, there is no more  $K_4Fe(CN)_6$  left to precipitate, and the region remains a thin, uncolored line of well defined boundaries with a thickness roughly two orders of magnitude smaller (down to  $\sim 300$  nm) than the spacing between the neighboring features in the stamp (25–250  $\mu\text{m}$ , Fig. 3b). Overall, the RD process transforms the original micropattern in the stamp into its Voronoi tessellation of nanoscale line thickness (Fig. 3c–d).

The stopping of RD fronts so close to one another and with such optically sharp boundaries is a result of a nonlinear dependence of the diffusion coefficients of the reacting species on the spatial location, and on the amount of precipitate present at this location. Specifically, the diffusion coefficient of the migrating  $[Fe(CN)_6]^{4-}$  ions (denoted henceforth as B) depends on the amount of precipitate (denoted C), while that of the metal cations (A) does not; at the same time, diffusion coefficients of all species decrease with depth since lower portions of the gelatin film are hydrated to a lesser extent than those close to the surface. Consequently, as the reaction (color) fronts approach one another, it gets increasingly harder for B to diffuse outwards—in other words, B is trapped between the fronts and cannot escape until they are within less than a micrometre of one another.

We briefly mention that modeling of this and related systems (*vide supra*) is somewhat challenging since the precipitation reaction is much faster than the transport of components. To circumvent this problem, the reaction terms in RD equations can be treated as precipitation sinks with a threshold determined by the solubility product,  $K_{sp}$ , and mathematically described by the Heaviside step function. The use of the Heaviside function implies that if the concentrations of ions are above  $K_{sp}$ , precipitation occurs instantaneously. For a reaction of stoichiometry  $nA + mB \rightarrow C \downarrow$ , the RD equations in nondimensionalized variables are:

$$\partial[A]/\partial\tau = D_A^{-1}\nabla D_A\nabla[A] - \delta_A\Theta([A]^n[B]^m - K_{sp})$$

$$\partial[B]/\partial\tau = D_B^{-1}\nabla D_B\nabla[B] - \delta_B\Theta([A]^n[B]^m - K_{sp})$$

$$\partial[C]/\partial\tau = \delta_C\Theta([A]^n[B]^m - K_{sp}),$$

with  $K_{sp} = ([A] - \delta_A)^n([B] - m\delta_A/n)^m$ ,  $\delta_B = n\delta_A/m$  and  $\delta_C = \delta_A/n$ . Numerical solutions of these equations are in excellent agreement with experimental observations.

In the context of applications, it is essential that the width of the clear lines and the spatial distribution of precipitate can be controlled by adjusting the concentrations and nature of reacting species as well as the dimensions of the stamped pattern. This control allowed us to fabricate high quality diffraction gratings with adjustable slit size as well as binary and gradient masks for photolithography (Fig. 3e–g). When used as masks, the colored portions of the films prepared with concentrated (1M)  $FeCl_3$  were completely opaque to UV radiation, and the developed photoresist had binary topography. In contrast, for less concentrated salts, especially in the  $CoCl_2/K_4Fe(CN)_6$  system, the intensity of transmitted

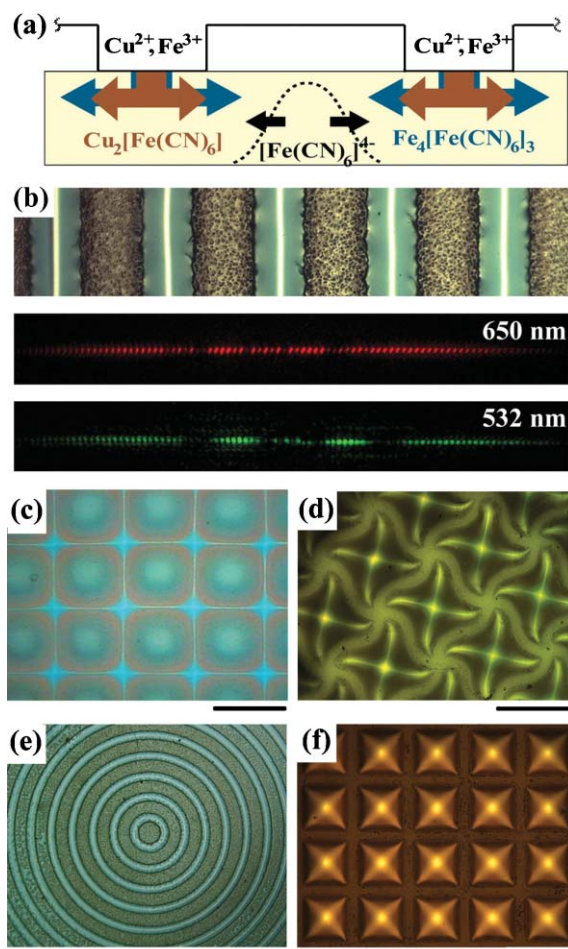


**Fig. 4** Simultaneous multicolor RD micropatterning. The scheme in (a) illustrates the experimental setup for patterning mixtures of salt solutions (here,  $CuCl_2$  and  $FeCl_3$ ) onto thin films of dry gelatin doped with  $K_4Fe(CN)_6$ . (b) The two-color micropattern of  $Fe_4[Fe(CN)_6]_3$  (blue) and  $Cu_2[Fe(CN)_6]$  (brown) precipitates diffracts red and green light differently. The stamped lines are 250  $\mu\text{m}$  wide and separated by 250  $\mu\text{m}$ . Pictures (c)–(f) show multicolor and/or color-gradient structures obtained by wet-stamping of different mixtures of salts from different stamp geometries: (c)  $CuCl_2/FeCl_3/CoCl_2$  (0.014 M : 0.31 M : 0.67 M) from a square array of circular dots; (d)  $CoCl_2/CuCl_2$  (5% : 5% w/w) from wavy lines on a square lattice; (e)  $FeCl_3/CuCl_2/Er(NO_3)_3$  (7% : 7% : 7% w/w) from concentric circles; (f)  $CoCl_2/FeCl_3/CuCl_2$  (5% : 5% : 5% w/w) from straight lines on a square lattice. Even for the same stamp geometry, micropatterns differing only in the relative amounts of salts can have drastically different appearances. Scale bars for (c)–(f) are 300  $\mu\text{m}$ .

radiation reflected the concentration gradient of the turquoise precipitate in the gel, and the developed photoresist had a continuously varying topography.<sup>11</sup>

## (ii) Multicolor patterning (Fig. 4)

In contrast to conventional micropatterning techniques, which are inherently binary, reaction–diffusion can be used to simultaneously micropattern surfaces with several chemicals at different locations.<sup>140</sup> An illustrative example of this capability is a two-color pattern shown in Fig. 4a which serves as a wave-selective diffraction grating (see Fig. 4b). To make

such a structure, a hydrogel stamp is soaked in a solution of two salts (*e.g.*,  $\text{FeCl}_3$  and  $\text{CuCl}_2$ ), each of which gives a colored precipitate with another salt (*e.g.*,  $\text{K}_4[\text{Fe}(\text{CN})_6]$ ) contained in the dry gelatin substrate. The separation of colors is the result of an intricate interplay between diffusion coefficients of ions in gelatin, their solubility products with respect to the common ion contained therein, and the local dehydration of agarose in the stamp's features. Once the stamp is in contact with the gel's surface, copper cations diffuse into gelatin more rapidly than iron cations—consequently they react with  $[\text{Fe}(\text{CN})_6]^{4-}$  first and give a layer of brown precipitate under every stamped feature. The iron cations enter a zone already depleted of  $\text{K}_4[\text{Fe}(\text{CN})_6]$ . Because the concentration of free  $\text{Fe}^{3+}$  in this zone is much higher than that of  $\text{Cu}^{2+}$ , iron cations experience a much higher concentration gradient in the plane of the gelatin film, and thus diffuse outwards from the features more rapidly than copper cations (despite lower value of the diffusion coefficient of  $\text{Fe}^{3+}$ ). In addition, the flux of copper

ions comes to a halt first, because it was initially higher than that of  $\text{Fe}^{3+}$ , and there are only finite amounts of both types of ions delivered from the stamp. The combination of these two effects leads the diffusion of iron ions to eventually “overtake” that of copper ions, thereby creating clean, blue zones of iron precipitate around the brown copper zones.

Patterns of colors other than blue and brown can be obtained by using different combinations of inorganic salts. Fig. 4b and c show surfaces patterned in two and even three colors using cobalt, copper, iron, and europium salts. Each of these patterns has different diffraction and/or light filtering characteristics.

### (iii) Multilevel surfaces and microdevices (Fig. 5)

When RD is *coupled* to the elastic properties of the medium, it can be used to transform local concentrations of reacting chemicals into surface elevations. With proper spatial encoding of the initial distribution of these chemicals, RD evolves a flat surface into a quasi three-dimensional one. We explored this property in a chemical system of silver nitrate (in the stamp) and potassium hexacyanoferrate (in the substrate) to make arrays of curved microlenses<sup>102</sup> as well as microfluidic passive mixer circuits.<sup>141</sup>

To make microlenses, RD is initiated from stamps patterned with an array of depressions in bas-relief (Fig. 5a). The precipitation reaction between silver cations (diffusing inwards from the contours of these depressions into gelatin) and  $[\text{Fe}(\text{CN})_6]^{4-}$  anions contained therein, results in a pronounced expansion of the gel; the degree of this expansion is (i) proportional to the amount of precipitate formed at a given location and (ii) decays monotonically with the distance from the features' edges. When the RD process comes to a halt, the surface of the gel is patterned with curvilinear depressions.

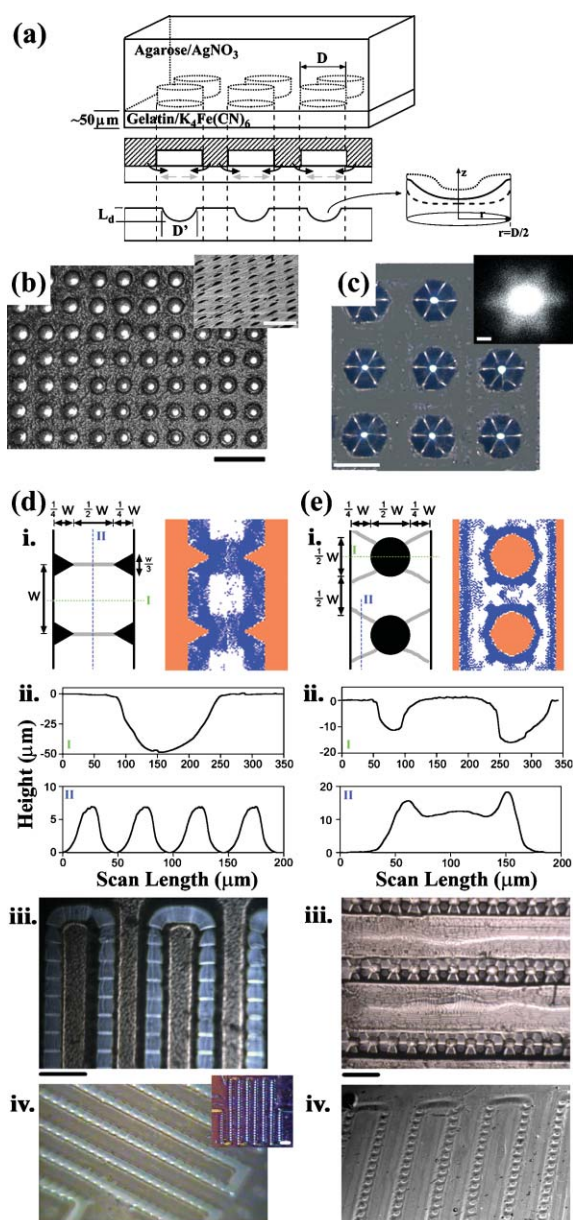


**Fig. 5** Microdevices *via* RD. The top scheme in (a) illustrates an agarose stamp with an array of depressions (of diameter,  $D$ ) in bas-relief that serve as a template for microlenses. The stamp is soaked in a solution of  $\text{AgNO}_3$  and applied onto a gel doped with  $\text{K}_4\text{Fe}(\text{CN})_6$ .  $\text{AgNO}_3$  diffuses (middle section) into the gelatin to react with the  $\text{K}_4\text{Fe}(\text{CN})_6$  and form a precipitate,  $\text{Ag}_4\text{Fe}(\text{CN})_6$ , that swells the gelatin. The bottom scheme is a section of the gelatin film after the stamp has been removed, with  $D'$  indicating the new diameter of the hemispherical feature and  $L_d$  denoting its height; the degree of swelling is proportional to the concentration of  $\text{Ag}_4\text{Fe}(\text{CN})_6$ . Arrays of microlenses shown in (b) and (c) were stamped from 10% w/w  $\text{AgNO}_3$  onto a gel with 1% w/w  $\text{K}_4\text{Fe}(\text{CN})_6$ : (b) an array ( $D = 50 \mu\text{m}$ ,  $D' \approx 45 \mu\text{m}$ ) of hemispherical lenses replicated into a transparent elastomer, poly (dimethyl siloxane); the focal length of each lens was measured to be  $75 \mu\text{m}$  (scale bars =  $200 \mu\text{m}$ ); (c) an array of hexagonal pyramids (scale bar =  $150 \mu\text{m}$ ), with the inset showing an image of a focal plane of the lenses in this array (scale bar =  $2 \mu\text{m}$ ). (d,e) Gel swelling can lead to complex surface topographies with uses in microfluidic devices. Triangular protrusions stamped in (d.i) lead to small, periodic ridges (lower profilogram in (d.ii)) running perpendicular to the length of a deeper microfluidic channel (upper profilogram in (d.ii)); stamped circles give rise to a complex, serpentine morphology used in caterpillar micromixers (e.i) and (e.ii). (d.iii–iv); (e.iii–iv) Both types of structures can be faithfully replicated into PDMS over large areas to give molds for microfluidic circuits. Scale bars in (d) and (e) correspond to  $300 \mu\text{m}$ .

Depending on the applied pattern, these depressions can be sections of a sphere (when RD was initiated from circles, Fig. 5b) or pyramidal (when initiated from polygonal contours, Fig. 5c). In both cases, the heights and curvatures of these microstructures can be controlled by the concentrations of the chemicals used. Importantly, the depressions can be easily replicated into optically transparent polymers to give large (up to 3 cm × 3 cm) arrays of regular microlenses with uses in imaging sensors,<sup>142</sup> optical limiters,<sup>143</sup> confocal microscopy,<sup>144</sup> and quantum computing systems.<sup>145</sup>

A similar concept of RD translating into gel swelling was used to prepare multilevel microfluidic circuits.<sup>141</sup> In microfluidics, mixing fluids that flow in a laminar fashion through narrow channels is difficult, and several devices have been proposed to achieve this goal.<sup>146</sup> One of the most efficient, passive mixers uses small ridges patterned at the bottom of the channel<sup>147</sup> to mix the fluids by the so-called chaotic advection mechanism.<sup>148,149</sup> While simple in concept, such structure is hard to fabricate and requires several microfabrication steps—RD can perform the same task in one step.

In our design, the initial conditions for the RD process (as before, determined by the geometry of the stamp), were given by contours of the channel from which silver cations migrated inwards, into the dry gel. The stamped regions (the background) swelled uniformly, so that the channels were depressions in an otherwise flat surface. The ridges in the channels were obtained by using stamps in which the side walls of the channels had either small protrusions (Fig. 5d–i) or features inside the channels (circles in Fig. 5e–i). The first type of design gave channels with regularly spaced ridges running across the channel (Fig. 5d.ii–iii) and of heights *ca.* 16% of the channel's depth; channels of very similar topographies have been shown to be excellent micromixers.<sup>150</sup> In the second design (Fig. 5e.ii–iii), the arrangement of ridges was more complex and was inspired by the caterpillar flow mixer developed by Ehrfeld and co-workers.<sup>151</sup> In both cases, gelatin molds were successfully replicated in PDMS demonstrating that they can be used as masters for actual devices (Fig. 5d,e.iv).

It is worth noting that the ridges in these designs are perpendicular to the directions of propagation of the reaction fronts originating from the patterned features. This directionality, uncommon to RD systems in which structures usually form parallel to the reaction front line, is a consequence of a complex sequence of reaction, diffusion, swelling and gel contraction. Also, at the locations of ridges, the silver hexacyanoferrate precipitate decomposes into colloidal silver oxide particles and regenerates hexacyanoferrate anions. Details of this interesting mechanism are described elsewhere;<sup>141</sup> we also note that a lattice-gas dynamics computer program to model these and other complex structures is available free of charge from our website.<sup>152</sup>

#### (iv) Periodic precipitation (PP) and nanostructured surfaces (Fig. 6)

Periodic precipitation reactions can generate multiple, discrete micro- or nanostructures (bands) from a single reaction source. In typical experimental arrangements, PP is propagated from simple geometries and the diffusion of ions into the gel

medium is accompanied by strong backflow/hydrodynamic effects.<sup>13</sup> Since the formation of PP bands requires purely diffusive transport of participating chemicals,<sup>153,154</sup> these hydrodynamic effects suppress the formation of patterns near the source of the outer electrolyte, and the first distinct bands observed outside of the uniform precipitation zone have macroscopic dimensions. WETS eliminates both of these limitations—indeed, the smallest bands we were able to resolve<sup>155</sup> were  $\sim 500$  nm wide (Fig. 6a), and the transport was diffusive to such a degree that it was even possible to controllably propagate the defects in the PP arrays.<sup>13</sup> (Fig. 6b)

The two-dimensional PP patterns are not only of interest in optics as diffraction gratings and planar Fresnel-like lenses<sup>103,104</sup> (Fig. 6c), but can also structure surfaces with nanoscopic waves of linearly increasing heights (Fig. 6d). This phenomenon follows from the fact that the forming bands collect all the mobile-phase precipitate from between each other, and that the amount of precipitate collected by band number  $n$  (counting in the direction of front propagation) is

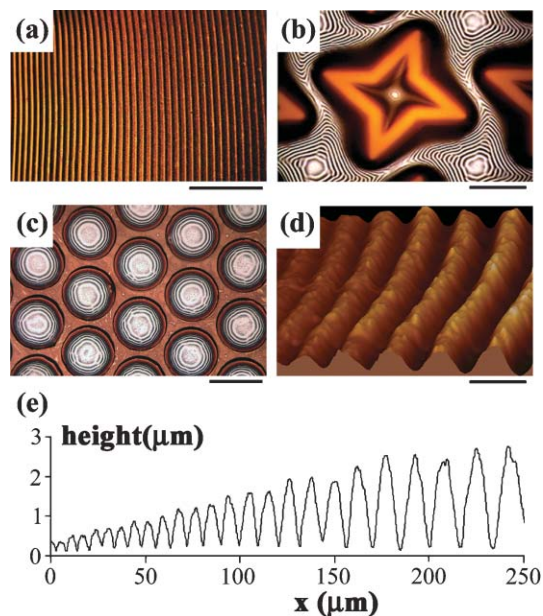


**Fig. 6** Surface micropatterning and nanostructuring using periodic precipitation (a) Submicrometre precipitation bands formed by diffusion of 60% (w/w) aqueous solution of  $\text{AgNO}_3$  into a dry gel. The gel was prepared by spin-coating (at 300 rpm) a 7.5% gelatin solution containing 1.5% of  $\text{K}_2\text{Cr}_2\text{O}_7$  and 1% KOH on glass, letting it dry for 2 days and irradiating it with 0.7 mW of 365 nm UV light for 18 s (scale bar: 25  $\mu\text{m}$ ). (b) Diffusion of 1M  $\text{AgNO}_3$  from a chiral star stamped pattern into a 36  $\mu\text{m}$  thick gelatin film doped with 5%  $\text{K}_2\text{Cr}_2\text{O}_7$  produces patterns in which wedge-shaped defects/dislocations propagate controllably along the diagonals of squares between the arms of the stamped stars (scale bar: 500  $\mu\text{m}$ ). (c) Optical micrograph of an array of planar Fresnel-like lenses (hexagonal arrangement,  $D = 600$   $\mu\text{m}$ ) produced by diffusion of a 15% (w/w)  $\text{AgNO}_3$  solution into a 10  $\mu\text{m}$  gelatin layer doped with  $\text{K}_2\text{Cr}_2\text{O}_7$ . The thickness of the bands increases with the distance from the boundary of the stamped circles, from several  $\mu\text{m}$  near the edge up to  $\sim 50$   $\mu\text{m}$  near the center (scale bar: 600  $\mu\text{m}$ ). (d) AFM image and (e) profilogram of a surface “nanobuckled” by PP rings (10%  $\text{AgNO}_3$ , 10%  $\text{K}_2\text{Cr}_2\text{O}_7$ ) of linearly increasing heights (scale bar: 10  $\mu\text{m}$ ).

proportional to its distance from the source,  $x_n$ .<sup>13</sup> In addition, the deformation of the surface is proportional to the local concentration of the precipitate. The heights of the waves increase in a regular fashion from tens of nanometres to several micrometres over a distance of couple hundred  $\mu\text{m}$  (Fig. 6e). The rate of increase can be modulated by adjusting the material properties of the gel medium (especially, cross-linking) as well as the concentrations of reacting species.

This example shows how powerful a nanofabrication tool RD can be. While in the case of microsystems described earlier, RD offered an *easier* way to structures that could, in principle, be meticulously fabricated by multistep photolithography, nanowaves could not be prepared by any fabrication technique currently known. These structures provide interesting test-beds for studying friction at small scales<sup>156</sup> as well as mechanical properties of cells spreading and moving on polymeric replicas of such gradient, ‘fakir surfaces’.<sup>157,158</sup> In particular, our laboratory is currently investigating how the cytoskeleton responds to nanoscale obstacles of increasing heights during cell motion.

### Structuring solids with RD (Fig. 7)

The usefulness of RD is not limited to modifying soft materials. We have successfully applied it as a basis of two versatile techniques to make microstructures of metals, glasses and crystals.

In the first application,<sup>159</sup> diffusional fluxes between a micropatterned gel and an aqueous plating solution direct the electroless deposition (reaction) of microstructured, 3D metal foils at the gel’s surface (Fig. 7a). The gel serves as a reservoir of catalytic Sn/Pd seeds characterized by exponentially-decaying size distribution and with mean particle radius  $R_{av} \sim 1.5$  nm. When this gel is placed in a plating solution, the seeds migrate towards its micropatterned surface, where they catalyze the reduction of metal cations from solution; the size of the particles that are presented at the surface determines the roughness of the deposited metal film. At the same time, the topography of this film depends on the local magnitudes of fluxes of the plating solution which, in turn, depend on the geometry of the microfeatures. Because the rate of metal deposition is directly proportional to the flux at the gel’s surface, the metal is plated most rapidly in places where the concentration gradients are steepest: deposition is fastest at the tops of the features (starting from the corners), and slowest at their bottoms (ending in the corners). These dependencies allow selective metallization of micropatterns to give either continuous (Fig. 7b), discontinuous or membrane-like (Fig. 7d) metal films which are useful in lightweight materials,<sup>160–165</sup> micro-waveguides,<sup>166,167</sup> and micro-/nanoelectronic devices.<sup>168,169</sup>

In the second approach<sup>170</sup> (Fig. 7e and f), reaction–diffusion is used to structure solid materials. Here, micropatterned hydrogel stamps are soaked in a reagent that dissolves/etches the solid. When the tops of the stamp’s features come into contact with the substrate, etching occurs at the interface between the two materials. This reaction decreases the concentration of the etchant and increases that of the reaction products near the surface; diffusion from/towards the bulk of

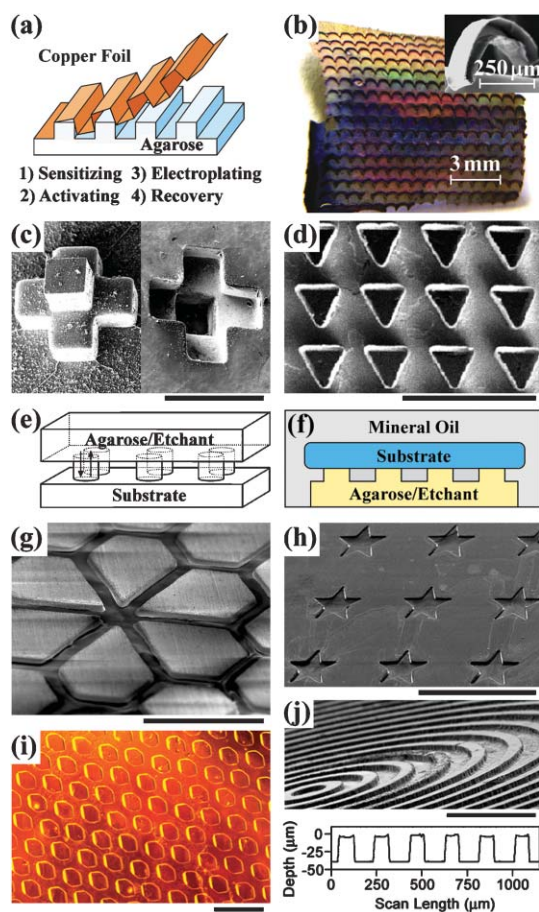


**Fig. 7** Structuring Solids with RD. (a) Experimental arrangement for the fabrication of microstructured copper foils. An agarose stamp patterned in bas-relief is soaked first in a sensitizing  $\text{Sn}^{2+}$  solution and then an activating  $\text{Pd}^{2+}$  solution to form catalytic seeds in the gel *via* RD. The stamp is then immersed in an electroless plating solution to create rugged copper foils at the gel/solution interface. The foils are recovered from the gel surface to produce either freestanding or polymer supported metallic microstructures. (b) Continuous free standing copper foil. (c) Front and back of a three dimensional cross. (d) Membrane-like structure created by controlling the diffusional fluxes at gel/solution interface. (e) Experimental schematic of a patterned hydrogel stamp etching into a solid substrate. Diffusive fluxes deliver the chemical etchant from the reservoir to the stamp/substrate interface while continuously removing the reaction products. (f) To etch hydrophilic surfaces, such as glass, it is necessary to reduce lateral etching due to capillary wetting by immersing both the substrate and the stamp in mineral oil. (g) Disjoint metal polygons created by etching through a  $40 \mu\text{m}$  copper film. (h) Clean, anisotropic etching of star-shaped wells in glass. (i) Chemical etching of calcium carbonate crystal. (j) Anisotropic etching of concentric circles in glass (top) and the corresponding profile (bottom). All scale bars are  $500 \mu\text{m}$  unless otherwise noted.

the stamp resupplies the former and clears away the latter. As etching progresses, the stamp melts into the solid anisotropically—that is, without lateral spreading of the etchant over the solid’s surface—to microstructure it with high-aspect ratio features. Overall, reaction–diffusion enables a versatile, maskless way of engraving microstructures into metals (Fig. 7g), glasses (Fig. 7h,j) and other solids (Fig. 7j).

The patterns can be made more complex (e.g., multilevel) by either consecutive stampings or by adding other chemicals to the stamp that react with the products of solid dissolution to change the directions of diffusional fluxes in the stamp.

## RD and sensing (Fig. 8)

In micro- and nanofabrication applications, it is desirable that reaction–diffusion leads to static structures (cf. Table 1). In contrast, both static and dynamic RD phenomena can be used for sensing. The idea here is to monitor the material or

chemical properties of one system by coupling it to an auxiliary RD process. Ideally, this process should amplify and translate small changes occurring in the system of interest into a visual RD readout.

### (i) Static sensing

In the case of static systems, one way to achieve such amplification is to stamp a connected network of micro-features onto a substrate to be sensed. This is illustrated in Fig. 8b, which shows two types of RD patterns emerging from

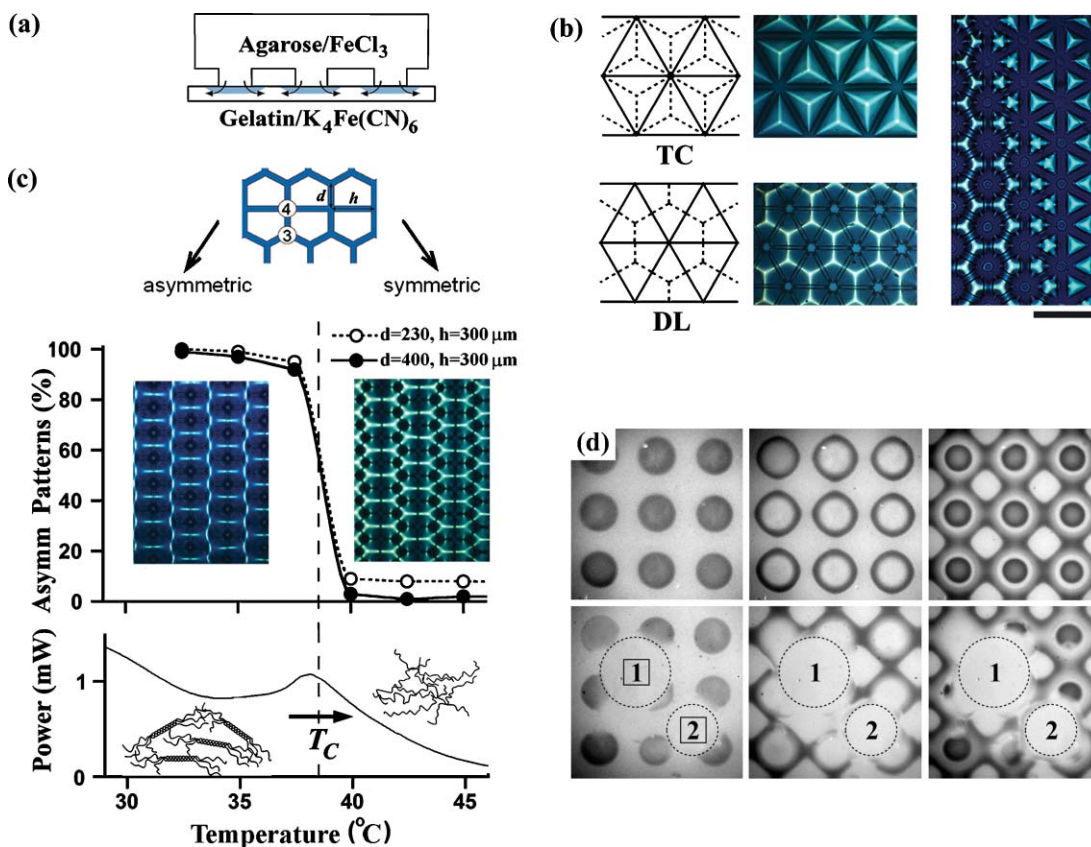


**Fig. 8** Sensing using reaction–diffusion. (a) The scheme illustrating WETS of a network of connected features (cf. Fig. 3a) (b) Two different color patterns (tile-centered, TC, and dual-lattice, DL, transformations) developed from identical stamped lattices of equilateral triangles on gels varying in thickness by  $\sim 1 \mu\text{m}$ . (scale bar =  $500 \mu\text{m}$ ) The right-most picture illustrates a sharp transition between the two geometric solutions on a gel of thickness continuously varying from  $\sim 10 \mu\text{m}$  in the top-right corner (TC solution) to  $\sim 35 \mu\text{m}$  in the bottom-left corner (DL solution). (c) Two different patterns emerging from a stamped network of pentagons (top picture) in response to the changes in the molecular structure of the substrate (here, gelatin doped with a hexacyanoferrate indicator). Depending on whether gelatin was prepared at a temperature,  $T$ , below or above the helix-to-coil transition temperature,  $T_C$ , asymmetric or symmetric RD solution is observed. In the asymmetric solution, the  $\text{Fe}^{3+}$  ions migrate from the three-fold nodes to the four-fold ones (marked by the numbers 3 and 4, respectively) prior to entering gelatin. Consequently, the color RD pattern propagates only from the four-fold nodes. In the symmetric solution, color patterns propagate from all nodes. The percentage of asymmetric solutions decreases abruptly as  $T$  approaches  $T_C \approx 39 \text{ }^\circ\text{C}$  (middle picture). The bottom picture shows a DSC scan of a gelatin/hexacyanoferrate solution undergoing a helix-to-coil transition at  $T_C$  equal to that of the crossover between asymmetric and symmetric RD patterns observed on the gel film. (d) Spatially distributed sensing of antioxidants in the Briggs–Rauscher chemical system. Here, all but one of the reagents are contained in a polyacrylamide gel sheet, into which the final component ( $\text{H}_2\text{O}_2$ ) was delivered *via* a micropatterned agarose stamp. The diffusing  $\text{H}_2\text{O}_2$  initiates oscillations only when its local concentration exceeds a critical value; therefore, oscillations begin earlier near the stamp features, creating a spatial gradient in the phase of oscillation. These phase gradients manifest themselves visually as chemical waves traveling outwards from the stamp features. The first series of pictures shows the evolution of nine “oscillators” in the absence of antioxidants. In the second series, an antioxidant (2,6-dihydroxybenzoic acid) was delivered to the PAA film from 1 mm agarose cubes before introducing  $\text{H}_2\text{O}_2$ . The concentration of antioxidant was 0.01M in cube 1 and 0.005M in cube 2; both cubes were applied for 20 s. Because antioxidants scavenge free radicals necessary for chemical oscillations, there are no waves in the regions influenced by the cubes. Note that region 1 is approximately twice as large as region 2, corresponding to the differences in antioxidant concentration.<sup>189</sup>

the same network placed onto porous substrates differing in thickness by  $\sim 1 \mu\text{m}$ .

In this system,<sup>171</sup> the substrate is doped with an indicator (typically, an inorganic salt), which reacts with the solute (ink) contained in the stamp to give a colored precipitate. Depending on the system's dimensions, the substrate "paper" drains different amounts of water from different parts of the network, thus establishing concentration gradients of the ink left therein. In response to these gradients, the ink redistributes itself within the network and enters the substrate either from the network's edges or from its nodes to produce different color patterns upon reaction with the indicator molecules. Because the degree of water outflow depends on, among other factors, the thickness of the substrate, RD patterns that emerge convey information about the paper's thickness.

The sensitivity of the micronetwork system can be further enhanced by using designs with two types of nodes.<sup>172</sup> In such cases, different patterns can emerge in response to minute changes in the macromolecular structure of the substrate. In Fig. 8c, we show how a helix-to-coil transition in a thin film of gelatin is sensed and directly visualized by switching between two types of RD tilings. Pattern crossover occurs at the temperature ( $T_C = 39 \text{ }^\circ\text{C}$ ) at which residual collagen-like helices unwind into random coils.

### (ii) Dynamic sensing

This mode of RD sensing has been used previously to detect antioxidants,<sup>173</sup> biologicals,<sup>174</sup> and light intensity<sup>175</sup> in bulk systems. Combining highly nonlinear oscillating reactions with geometrical microconfinement offered by a WETS-like approach allows extension of this method to spatially-distributed sensing—that is, sensing, in which the substrate is patterned with a regular array of oscillating elements, each of which provides a sensing "pixel". For example, Fig. 8d demonstrates spatially distributed detection of antioxidants using a micropatterned array of Briggs–Rauscher oscillators.

### Conclusions and outlook

In summary, we have described a straightforward experimental method based on simple inorganic chemistries that allows precise control of reaction–diffusion processes at small scales, and provides a facile route to complex micro- and nanostructures. All applications of WETS and related techniques we outlined are based on two-dimensional microgeometries from which reactions are initiated. While these planar systems can certainly be extended further to different soft-matter media (where effects of pore size, degree of crosslinking or chirality need to be considered) and to RD mechanisms based on small organic molecules, polymers or even nanoparticles, they are only precursors to three-dimensional, functional micro- and nanodevices, which we consider the ultimate goal of our work. The extension from two to three dimensions will very likely rely on self-assembly, in which building blocks carrying chemical reagents would first come together in a programmed fashion, and would then exchange and react their contents to build structures and/or perform desired tasks. Such self-organizing RD ensembles would rely on the use of soft/porous materials, and on surface chemistries that would enable

selective recognition of various types of pieces. In addition, if the assemblies were to perform several mechanical functions (intelligent systems), they should be reconfigurable and

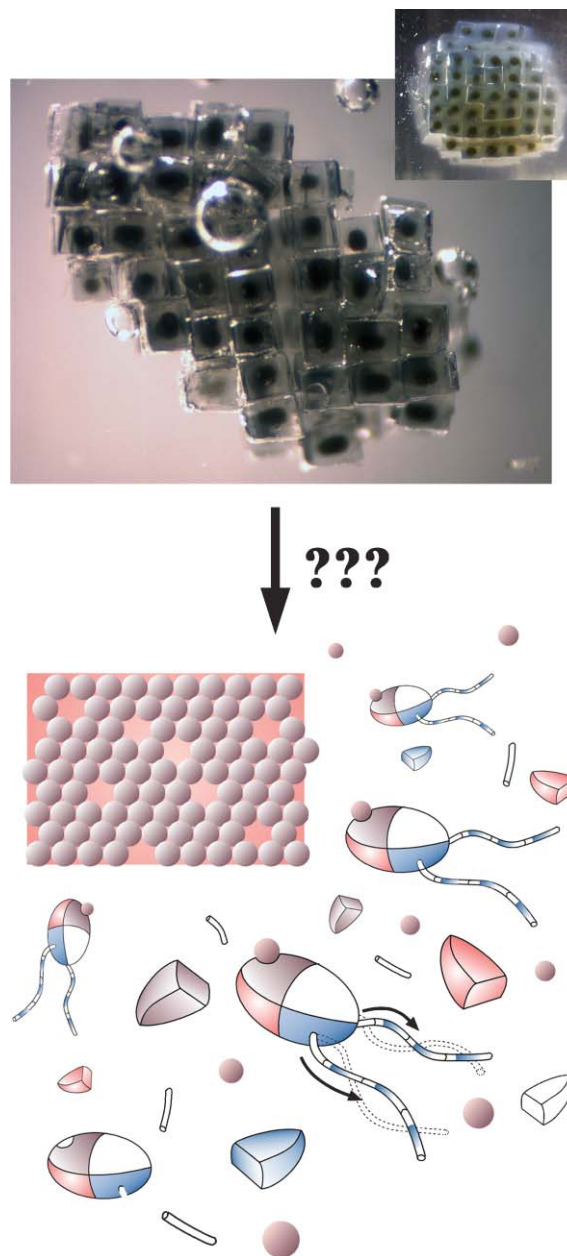


**Fig. 9** From toy models of self-assembling RD systems to real nanomachines. The top picture shows a collection of  $500 \mu\text{m}$  agarose cubes having metallic cores developed *inside* by reaction–diffusion and self-assembly into a larger, static structure. The insert shows the final, fully ordered state. The bottom picture is an artistic vision of dynamic, self-assembling nanomachines, each carrying a microsphere cargo to be deposited onto a growing colloidal array. Each nanomachine is powered by reaction–diffusion waves (blue bands) running synchronously along their "legs" (in the direction of the arrows), and is guided onto the array by a chemotactic attraction of its red "belly" towards the array's background (emitting red attractants). The design of these organisms was inspired by *Chlamydia* algae. The question marks next to the arrow express our current uncertainty of how to progress from simple "toy" models to truly intelligent assemblies based on a synergistic combination of self-assembly and reaction–diffusion processes.

responsive to external stimuli, this, in turn, necessitates a choice in the chemistry which can be addressed by external fields (magnetic,<sup>176</sup> electric<sup>177</sup> or optical<sup>178</sup>). To realize this vision, the experimental effort should be accompanied by theoretical studies of the principles that govern self-assembly outside thermodynamic equilibrium and on different length scales.<sup>179,180</sup>

There are no fundamental limitations why the ambitious goals we outlined could not be achieved. Indeed, the existence of living cells, the ultimate examples of three-dimensional RD nanosystems, encourages this view. How to get from the 'toy' models we can currently make to artificial cells (Fig. 9) depends only on our creativity in how to control reaction and diffusion at very small scales.

**Bartosz A. Grzybowski,\* Kyle J. M. Bishop, Christopher J. Campbell, Marcin Fialkowski and Stoyan K. Smoukov**

*Department of Chemical and Biological Engineering and The Northwestern Institute of Complex Systems, 2145 Sheridan Roadl TECH E136, Evanston, IL 60208, USA*

## References

- R. E. Liesegang, *Naturwiss. Wochenschr.*, 1896, **11**, 353–363.
- D. A. W. Thompson, *On Growth and Form*, Cambridge University Press, Cambridge, UK, 1992.
- P. Ball, *The Self-Made Tapestry: Pattern Formation in Nature*, Oxford University Press, New York, 1999.
- M. C. Cross and P. C. Hohenberg, *Rev. Mod. Phys.*, 1993, **65**, 851–1112.
- I. R. Epstein and K. Showalter, *J. Phys. Chem.*, 1996, **100**, 13132–13147.
- A. M. Turing, *Philos. Trans. R. Soc. London, Ser. B*, 1952, **237**, 37–72.
- G. Nicolis, I. Prigogine, *Self-organization in Nonequilibrium Systems: From Dissipative Structures to Order Through Fluctuations*, Wiley, New York, 1977.
- B. Hess and A. Mikhailov, *Science*, 1994, **264**, 223–224.
- A. J. Koch and H. Meinhardt, *Rev. Mod. Phys.*, 1994, **66**, 1481–1507.
- J. Crank, *The Mathematics of Diffusion*, Clarendon Press, Oxford, 2nd edn., 1975.
- C. J. Campbell, M. Fialkowski, R. Klajn, I. T. Bensemann and B. A. Grzybowski, *Adv. Mater.*, 2004, **16**, 1912–1917.
- H. S. Fogler, *Elements of Chemical Reaction Engineering*, Prentice-Hall, Englewood Cliffs, NJ, 3rd edn., 1998.
- I. T. Bensemann, M. Fialkowski and B. A. Grzybowski, *J. Phys. Chem. B*, 2005, **109**, 2774–2778.
- V. Castets, E. Dulos, J. Boissonade and P. Dekepper, *Phys. Rev. Lett.*, 1990, **64**, 2953–2956.
- Oscillations and Traveling Waves in Chemical Systems*, ed. R. J. Field and M. Burger, Wiley, New York, 1985.
- Calcium Waves, Gradients and Oscillations*, ed. G. R. Bock, and K. Ackrill Vol. 188, J. Wiley & Sons, New York, 1995.
- R. A. Fisher, *Ann. Eugen.*, 1937, **7**, 355–369.
- E. E. Holmes, M. A. Lewis, J. E. Banks and R. R. Veit, *Ecology*, 1994, **75**, 17–29.
- V. Mendez and J. E. Lebot, *Phys. Rev. E: Stat. Phys., Plasmas, Fluids, Relat. Interdiscip. Top.*, 1997, **56**, 6557–6563.
- D. Cartin and G. Khanna, *Phys. Rev. E: Stat. Phys., Plasmas, Fluids, Relat. Interdiscip. Top.*, 2002, **65**, 16120.
- S. A. Kauffman, R. M. Shymko and K. Trabert, *Science*, 1978, **199**, 259–270.
- R. E. Dolmetsch, K. L. Xu and R. S. Lewis, *Nature*, 1998, **392**, 933–936.
- E. A. Newman and K. R. Zahs, *Science*, 1997, **275**, 844–847.
- S. V. Straub, D. R. Giovannucci and D. I. Yule, *J. Gen. Physiol.*, 2000, **116**, 547–559.
- P. J. Garrahan and A. F. Rega, in *Intracellular calcium regulation*, ed. F. Bronner, Wiley-Liss, New York, 1990, 271–303.
- K. G. Baimbridge, M. R. Celio and J. H. Rogers, *Trends Neurosci.*, 1992, **15**, 303–308.
- J. H. Exton, *Physiol. Rev.*, 1997, **77**, 303–320.
- C. L. Farnsworth, N. W. Freshney, L. B. Rosen, A. Ghosh, M. E. Greenberg and L. A. Feig, *Nature*, 1995, **376**, 524–527.
- P. P. Dzeja and A. Terzic, *J. Exp. Biol.*, 2003, **206**, 2039–2047.
- J. G. Reich and E. E. Sel'kov, *Energy Metabolism of the Cell: a Theoretical Treatise*, Academic Press, New York, 1981.
- J. Tabony, N. Glade, J. Demongeot and C. Papaseit, *Langmuir*, 2002, **18**, 7196–7207.
- C. M. Gray, P. König, A. K. Engel and W. Singer, *Nature*, 1989, **338**, 334–337.
- D. Terman and D. L. Wang, *Physica D*, 1995, **81**, 148–176.
- M. A. Dahlem and S. C. Müller, *Ann. Phys. (Leipzig)*, 2004, **13**, 442–449.
- B. Hess, *Naturwissenschaften*, 2000, **87**, 199–211.
- A. Garfinkel, Y. H. Kim, O. Voroshilovsky, Z. L. Qu, J. R. Kil, M. H. Lee, H. S. Karagueuzian, J. N. Weiss and P. S. Chen, *Proc. Natl. Acad. Sci. USA*, 2000, **97**, 6061–6066.
- S. A. Newman, *Trends Genet.*, 1988, **4**, 329–332.
- S. A. Newman and H. L. Frisch, *Science*, 1979, **205**, 662–668.
- C. M. Leonard, H. M. Fuld, D. A. Frenz, S. A. Downie, J. Massague and S. A. Newman, *Dev. Biol.*, 1991, **145**, 99–109.
- S. Camazine, *Self-Organization in Biological Systems*, Princeton University Press, Princeton, NJ, 2001, ch. 8.
- E. O. Budrene and H. C. Berg, *Nature*, 1991, **349**, 630–633.
- E. O. Budrene and H. C. Berg, *Nature*, 1995, **376**, 49–53.
- S. Kondo and R. Asai, *Nature*, 1995, **376**, 765–768.
- T. X. Jiang, R. B. Wideltz, W. M. Shen, P. Will, D. Y. Wu, C. M. Lin, H. S. Jung and C. M. Chuong, *Int. J. Dev. Biol.*, 2004, **48**, 117–135.
- S. Kondo, *Genes Cells*, 2002, **7**, 535–541.
- M. B. Short, J. C. Baygents, J. W. Beck, D. A. Stone, R. S. Toomey and R. E. Goldstein, *Phys. Rev. Lett.*, 2005, **94**, 18501.
- C. S. Haase, J. Chadam, D. Feinn and P. Ortoleva, *Science*, 1980, **209**, 272–274.
- C. J. Allegre, A. Provost and C. Jaupart, *Nature*, 1981, **294**, 223–228.
- R. J. Reeder, R. O. Fagioli and W. J. Meyers, *Earth-Sci. Rev.*, 1990, **29**, 39–46.
- B. W. D. Yardley, C. A. Rochelle, A. C. Barnicoat and G. E. Lloyd, *Mineral. Mag.*, 1991, **55**, 357–365.
- H. J. Krug, K. H. Jacob and S. Dietrich, in *Fractals and Dynamic Systems in Geoscience*, ed. J.H. Kruhl and L.-O. Renftel, Springer-Verlag, Berlin, New York, 1994.
- P. J. Heaney and A. M. Davis, *Science*, 1995, **269**, 1562–1565.
- M. Flicker and J. Ross, *J. Chem. Phys.*, 1974, **60**, 3458–3465.
- S. C. Müller and J. Ross, *J. Phys. Chem. A*, 2003, **107**, 7997–8008.
- P. Hantz, *Phys. Chem. Chem. Phys.*, 2002, **4**, 1262–1267.
- R. Sultan, P. Ortoleva, F. Depasquale and P. Tartaglia, *Earth-Sci. Rev.*, 1990, **29**, 163–173.
- R. F. Sultan, N. K. Al-Kassem, A. A. H. Sultan and N. M. Salem, *Phys. Chem. Chem. Phys.*, 2000, **2**, 3155–3162.
- Glossary of Geology*, ed. R. L. Bates and J. A. Jackson American Geological Institute, Alexandria, VA., 3rd edn., 1987.
- B. Chopard, H. J. Herrmann and T. Vicsek, *Nature*, 1991, **353**, 409–412.
- H. E. Stanley, A. Bunde, S. Havlin, J. Lee, E. Roman and S. Schwarzer, *Physica A*, 1990, **168**, 23–48.
- T. A. Witten and L. M. Sander, *Phys. Rev. Lett.*, 1981, **47**, 1400–1403.
- A.-L. Barabási and H. E. Stanley, *Fractal Concepts in Surface Growth*, Cambridge University Press, Cambridge, 1995.
- D. Grier, E. Benjacob, R. Clarke and L. M. Sander, *Phys. Rev. Lett.*, 1986, **56**, 1264–1267.
- J. Kertesz and T. Vicsek, *J. Phys. A: Math. Gen.*, 1986, **19**, L257–L262.
- J. Nittmann and H. E. Stanley, *J. Phys. A: Math. Gen.*, 1987, **20**, L1185–L1191.
- J. Nittmann, G. Daccord and H. E. Stanley, *Nature*, 1985, **314**, 141–144.
- V. A. Bogoyavlenskiy, *Phys. Rev. E: Stat. Phys., Plasmas, Fluids, Relat. Interdiscip. Top.*, 2001, **64**, 66303.

- 68 B. P. Belousov, *A Periodic Reaction and its Mechanism*, Medgiz, Moscow, 1958.
- 69 I. R. Epstein, *An Introduction to Nonlinear Chemical Dynamics: Oscillations, Waves, Patterns, and Chaos*, Oxford University Press, New York, 1998.
- 70 T. S. Briggs and W. C. Rauscher, *J. Chem. Ed.*, 1973, **50**, 496–496.
- 71 A. N. Zaikin and A. M. Zhabotinsky, *Nature*, 1970, **225**, 535–537.
- 72 K. Showalter, *J. Phys. Chem.*, 1981, **85**, 440–447.
- 73 A. Hanna, A. Saul and K. Showalter, *J. Am. Chem. Soc.*, 1982, **104**, 3838–3844.
- 74 P. Dekepper, I. R. Epstein, K. Kustin and M. Orban, *J. Phys. Chem.*, 1982, **86**, 170–171.
- 75 A. P. Munuzuri and M. Markus, *Phys. Rev. E: Stat. Phys., Plasmas, Fluids, Relat. Interdiscip. Top*, 1997, **55**, R33–R35.
- 76 A. P. Munuzuri, M. Dolnik, A. M. Zhabotinsky and I. R. Epstein, *J. Am. Chem. Soc.*, 1999, **121**, 8065–8069.
- 77 M. Pornprompanya, S. C. Muller and H. Sevcikova, *Chem. Phys. Lett.*, 2003, **375**, 364–368.
- 78 K. Showalter and R. M. Noyes, *J. Am. Chem. Soc.*, 1976, **98**, 3728–3731.
- 79 K. Showalter, R. M. Noyes and H. Turner, *J. Am. Chem. Soc.*, 1979, **101**, 7463–7469.
- 80 A. T. Winfree, *Science*, 1973, **181**, 937–939.
- 81 P. M. Sutcliffe and A. T. Winfree, *Phys. Rev. E: Stat. Phys., Plasmas, Fluids, Relat. Interdiscip. Top*, 2003, **68**, 16218.
- 82 U. Storb, C. R. Neto, M. Bar and S. C. Muller, *Phys. Chem. Chem. Phys.*, 2003, **5**, 2344–2353.
- 83 R. Imbihl and G. Ertl, *Chem. Rev.*, 1995, **95**, 697–733.
- 84 P. Hugo, *Ber. Bunsen-Ges. Phys. Chem.*, 1970, **74**, 121–127.
- 85 H. Beusch, E. Wicke and P. Fieguth, *Chem.-Ing.-Tech.*, 1972, **44**, 445–451.
- 86 G. Ertl, *Science*, 1991, **254**, 1750–1755.
- 87 M. Ehsasi, C. Seidel, H. Ruppender, W. Drachsel, J. H. Block and K. Christmann, *Surf. Sci.*, 1989, **210**, L198–L208.
- 88 S. Fuchs, T. Hahn and H. G. Lintz, *Chem. Eng. Proc.*, 1994, **33**, 363–369.
- 89 S. Wehner, F. Baumann, M. Ruckdeschel and J. Kuppers, *J. Chem. Phys.*, 2003, **119**, 6823–6831.
- 90 J. E. Zuniga and D. Luss, *J. Catal.*, 1978, **53**, 312–320.
- 91 W. Adlhoch, H. G. Lintz and T. Weisker, *Surf. Sci.*, 1981, **103**, 576–585.
- 92 J. Siera, P. Cobden, K. Tanaka and B. E. Nieuwenhuys, *Catal. Lett.*, 1991, **10**, 335–342.
- 93 M. F. H. vanTol, A. Gielbert and B. E. Nieuwenhuys, *Catal. Lett.*, 1992, **16**, 297–309.
- 94 H. T. Wang, Z. B. Wang, L. M. Huang, A. Mitra and Y. S. Yan, *Langmuir*, 2001, **17**, 2572–2574.
- 95 K. Krischer, N. Mazouz and P. Grauel, *Angew. Chem. Int. Ed.*, 2001, **40**, 851–869.
- 96 I. Lengyel, S. Kadar and I. R. Epstein, *Science*, 1993, **259**, 493–495.
- 97 J. D. Murray, *Mathematical Biology*, Springer-Verlag, New York, 2nd, corr. edn., 1993.
- 98 Q. Ouyang and H. L. Swinney, *Nature*, 1991, **352**, 610–612.
- 99 R. Kapral and K. Showalter, *Chemical Waves and Patterns*, Kluwer Academic Publishers, Boston, 1995.
- 100 R. J. Field, R. M. Noyes and E. Koros, *J. Am. Chem. Soc.*, 1972, **94**, 8649–8664.
- 101 R. J. Field and R. M. Noyes, *J. Chem. Phys.*, 1974, **60**, 1877–1884.
- 102 C. J. Campbell, E. Baker, M. Fialkowski and B. A. Grzybowski, *Appl. Phys. Lett.*, 2004, **85**, 1871–1873.
- 103 H. Li and X. Huang, in *Micromachining and Microfabrication Process Technology VII*, ed. J.M. Karam and J. Yasaitis, SPIE, Bellingham, WA, 2001, 4557471–476.
- 104 C. J. Campbell, E. Baker, M. Fialkowski, A. Bitner, S. K. Smouk and B. A. Grzybowski, *J. Appl. Phys.*, 2005, DOI: 10.1063/1.1899757.
- 105 D. B. Glazier, D. P. Murphy, K. B. Cummings and F. A. Morrow, *J. Urol.*, 1997, **157**, 940–941.
- 106 J. E. Krueger, T. S. Corwin, R. Corwin and M. H. Saboorian, *J. Urol.*, 2000, **163**, 540–541.
- 107 N. Kumar and S. Jain, *Acta Cytol.*, 2000, **44**, 429–432.
- 108 I. Misselevich and J. H. Boss, *Int. J. Dermatol.*, 1999, **38**, 954–955.
- 109 K. H. Ng and C. H. Siar, *J. Laryngol. Otol.*, 1996, **110**, 757–762.
- 110 A. Padwell, *Br. J. Ophthalmol.*, 1995, **79**, 706–707.
- 111 P. L. Perrotta, F. W. Ginsburg, C. I. Siderides and V. Parkash, *Int. J. Gynecol. Pathol.*, 1998, **17**, 358–362.
- 112 H. G. Purwins, C. Radehaus and J. Berkemeier, *Z. Naturforsch., Sect. A*, 1988, **43**, 17–29.
- 113 A. L. Zanin, A. W. Liehr, A. S. Moskalenko and H. G. Purwins, *Appl. Phys. Lett.*, 2002, **81**, 3338–3340.
- 114 E. L. Gurevich, A. L. Zanin, A. S. Moskalenko and H. G. Purwins, *Phys. Rev. Lett.*, 2003, **91**, 154501.
- 115 A. L. Zanin, E. L. Gurevich, A. S. Moskalenko, H. U. Bodeker and H. G. Purwins, *Phys. Rev. E: Stat. Phys., Plasmas, Fluids, Relat. Interdiscip. Top*, 2004, **70**, 36202.
- 116 Y. A. Astrov, L. M. Portsel, S. P. Teperick, H. Willebrand and H. G. Purwins, *J. Appl. Phys.*, 1993, **74**, 2159–2166.
- 117 L. M. Portsel, Y. A. Astrov, I. Reimann, E. Ammelt and H. G. Purwins, *J. Appl. Phys.*, 1999, **85**, 3960–3965.
- 118 J. H. R. Kim, H. Maurer, Y. A. Astrov, M. Bode and H. G. Purwins, *J. Comput. Phys.*, 2001, **170**, 395–414.
- 119 S. J. Shuai and J. X. Wang, *Chem. Eng. J.*, 2004, **100**, 95–107.
- 120 B. Marwaha, S. Sundarram and D. Luss, *J. Phys. Chem. B*, 2004, **108**, 14470–14476.
- 121 A. Jaree, R. R. Hudgins, H. M. Budman, P. L. Silveston, V. Z. Yakhnin and M. Menzinger, *Ind. Eng. Chem. Res.*, 2003, **42**, 1662–1673.
- 122 A. Jaree, R. R. Hudgins, H. Budman, P. L. Silveston, V. Yakhnin and M. Menzinger, *Chem. Eng. Sci.*, 2003, **58**, 833–839.
- 123 *Handbook of Microlithography, Micromachining, and Microfabrication*, ed. P. Rai-Choudhury, SPIE Optical Engineering Press, Bellingham, WA, 1997.
- 124 L. F. Thompson and R. E. Kerwin, *Annu. Rev. Mater. Sci.*, 1976, **6**, 267–301.
- 125 Y. N. Xia and G. M. Whitesides, *Angew. Chem. Int. Ed.*, 1998, **37**, 551–575.
- 126 B. Michel, A. Bernard, A. Bietsch, E. Delamarche, M. Geissler, D. Juncker, H. Kind, J. P. Renault, H. Rothuizen, H. Schmid, P. Schmidt-Winkel, R. Stutz and H. Wolf, *IBM J. Res. Dev.*, 2001, **45**, 697–719.
- 127 N. B. Larsen, H. Biebuyck, E. Delamarche and B. Michel, *J. Am. Chem. Soc.*, 1997, **119**, 3017–3026.
- 128 E. Delamarche, C. Donzel, F. S. Kamounah, H. Wolf, M. Geissler, R. Stutz, P. Schmidt-Winkel, B. Michel, H. J. Mathieu and K. Schaumburg, *Langmuir*, 2003, **19**, 8749–8758.
- 129 D. W. L. Tolfree, *Rep. Prog. Phys.*, 1998, **61**, 313–351.
- 130 G. M. Wallraff and W. D. Hinsberg, *Chem. Rev.*, 1999, **99**, 1801–1821.
- 131 C. C. Cunningham, T. P. Stossel and D. J. Kwiatkowski, *Science*, 1991, **251**, 1233–1236.
- 132 C. A. Parent and P. N. Devreotes, *Science*, 1999, **284**, 765–770.
- 133 W. Suchanek and M. Yoshimura, *J. Mater. Res.*, 1998, **13**, 94–117.
- 134 W. W. Minuth, M. Sittinger and S. Kloth, *Cell Tissue Res.*, 1998, **291**, 1–11.
- 135 P. K. Manhart and R. Blankenbecler, *Opt. Eng.*, 1997, **36**, 1607–1621.
- 136 H. W. Ren and S. T. Wu, *Appl. Phys. Lett.*, 2002, **81**, 3537–3539.
- 137 C. Sachs, M. Hildebrand, S. Volkening, J. Winterlin and G. Ertl, *Science*, 2001, **293**, 1635–1638.
- 138 C. Sachs, M. Hildebrand, S. Volkening, J. Winterlin and G. Ertl, *J. Chem. Phys.*, 2002, **116**, 5759–5773.
- 139 M. Fialkowski, C. J. Campbell, I. T. Bensemann and B. A. Grzybowski, *Langmuir*, 2004, **20**, 3513–3516.
- 140 R. Klajn, M. Fialkowski, I. T. Bensemann, A. Bitner, C. J. Campbell, K. Bishop, S. Smouk and B. A. Grzybowski, *Nat. Mater.*, 2004, **3**, 729–735.
- 141 C. J. Campbell, R. Klajn, M. Fialkowski and B. A. Grzybowski, *Langmuir*, 2005, **21**, 418–423.
- 142 N. Daemen and H. L. Peek, *Philips J. Res.*, 1994, **48**, 281–297.
- 143 M. V. Gryaznova, V. V. Danilov, M. A. Belyaeva, P. A. Shakhverdov, O. V. Chistyakova and A. I. Khrebtov, *Opt. Spectrosc.*, 2002, **92**, 614–618.
- 144 E. M. McCabe, C. M. Taylor and L. Yang, *Proc. SPIE-Int. Soc. Opt. Eng.*, 2002, **4876**, 1–10.
- 145 R. Dumke, M. Volk, T. Muther, F. B. J. Buchkremer, G. Birkel and W. Ertmer, *Phys. Rev. Lett.*, 2002, **89**, 97903.

- 146 C. J. Campbell and B. A. Grzybowski, *Philos. Trans. R. Soc. London Ser. A*, 2004, **362**, 1069–1086.
- 147 A. D. Stroock, S. K. W. Dertinger, A. Ajdari, I. Mezic, H. A. Stone and G. M. Whitesides, *Science*, 2002, **295**, 647–651.
- 148 H. Aref, *J. Fluid Mech.*, 1984, **143**, 1–21.
- 149 J. M. Ottino, *The kinematics of Mixing: Stretching, Chaos, and Transport*, Cambridge University Press, Cambridge, 1989.
- 150 A. D. Stroock, S. K. Dertinger, G. M. Whitesides and A. Ajdari, *Anal. Chem.*, 2002, **74**, 5306–5312.
- 151 W. Ehrfeld, J. Hartmass, V. Hessel, S. Kiesewalter and H. Lowe, in *Proceedings of the Micro total analysis systems 2000*, ed. A. van den Berg, W. Olthuis and P. Bergveld, Kluwer Academic Publishers, Boston, MA, 2000, 33–40.
- 152 <http://dysa.northwestern.edu>.
- 153 H. K. Henisch, *Periodic Precipitation: a Microcomputer Analysis of Transport and Reaction Processes in Diffusion Media, with Software Development*, Pergamon, Oxford, 1st edn., 1991.
- 154 T. Antal, M. Droz, J. Magnin, Z. Racz and M. Zrinyi, *J. Chem. Phys.*, 1998, **109**, 9479–9486.
- 155 S. K. Smoukov, A. Bitner and B. A. Grzybowski, *Nano Lett.*, 2005 submitted.
- 156 I. L. Singer, *J. Vac. Sci. Technol. A-Vac. Surf. Films*, 1994, **12**, 2605–2616.
- 157 J. L. Tan, J. Tien, D. M. Pirone, D. S. Gray, K. Bhadriraju and C. S. Chen, *Proc. Natl. Acad. Sci. USA*, 2003, **100**, 1484–1489.
- 158 X. Y. Jiang, S. Takayama, X. P. Qian, E. Ostuni, H. K. Wu, N. Bowden, P. LeDuc, D. E. Ingber and G. M. Whitesides, *Langmuir*, 2002, **18**, 3273–3280.
- 159 S. K. Smoukov, K. J. M. Bishop, C. J. Campbell and B. A. Grzybowski, *Adv. Mater.*, 2005, **17**, 751–755.
- 160 J. Zaumseil, M. A. Meitl, J. W. P. Hsu, B. R. Acharya, K. W. Baldwin, Y. L. Loo and J. A. Rogers, *Nano Lett.*, 2003, **3**, 1223–1227.
- 161 J. L. Yan, Y. Du, J. F. Liu, W. D. Cao, S. H. Sun, W. H. Zhou, X. R. Yang and E. K. Wang, *Anal. Chem.*, 2003, **75**, 5406–5412.
- 162 I. Rodriguez, P. Spicar-Mihalic, C. L. Kuyper, G. S. Fiorini and D. T. Chiu, *Anal. Chim. Acta*, 2003, **496**, 205–215.
- 163 D. Dobrev, R. Neumann, N. Angert and J. Vetter, *Appl. Phys. A-Mater. Sci. Process.*, 2003, **76**, 787–790.
- 164 Y. S. Cheng and K. L. Yeung, *J. Membr. Sci.*, 1999, **158**, 127–141.
- 165 S. T. Brittain, Y. Sugimura, O. J. A. Schueller, A. G. Evans and G. M. Whitesides, *J. Microelectromech. Syst.*, 2001, **10**, 113–120.
- 166 I. C. E. Turcu, R. M. Allot, C. M. Mann, C. Reeves, I. N. Ross, N. Lisi, B. J. Maddison, S. W. Moon, P. Prewett, J. T. M. Stevenson, A. W. S. Ross, A. M. Gundlach, B. Koek, P. Mitchell, P. Anastasi, C. McCoard and N. S. Kim, *J. Vac. Sci. Technol. B*, 1997, **15**, 2495–2502.
- 167 S. Koike, F. Shimokawa, T. Matsuura and H. Takahara, *IEEE Trans. Comp. Pack. Manuf. Technol. B*, 1996, **19**, 124–130.
- 168 T. Osaka, N. Takano and T. Yokoshima, *Surf. Coat. Technol.*, 2003, **169**, 1–7.
- 169 Y. Shacham-Diamand, A. Inberg, Y. Sverdlov, V. Bogush, N. Croitoru, H. Moscovich and A. Freeman, *Electrochim. Acta*, 2003, **48**, 2987–2996.
- 170 S. K. Smoukov, K. J. M. Bishop, R. Klajn, C. J. Campbell and B. A. Grzybowski, *Adv. Mater.*, 2005, DOI: 10.1002/adma.200402086.
- 171 A. Bitner, M. Fialkowski and B. A. Grzybowski, *J. Phys. Chem. B*, 2004, **108**, 19904–19907.
- 172 A. Bitner, M. Fialkowski, S. K. Smoukov, C. J. Campbell and B. A. Grzybowski, *J. Am. Chem. Soc.*, 2005, DOI: 10.1021/ja051128p.
- 173 R. Cervellati, K. Honer, S. D. Furrow, C. Neddens and S. Costa, *Helv. Chim. Acta*, 2001, **84**, 3533–3547.
- 174 M. Eigen and R. Rigler, *Proc. Natl. Acad. Sci. USA*, 1994, **91**, 5740–5747.
- 175 H. Brandtstadter, M. Braune, I. Schebesch and H. Engel, *Chem. Phys. Lett.*, 2000, **323**, 145–154.
- 176 B. A. Grzybowski, H. A. Stone and G. M. Whitesides, *Nature*, 2000, **405**, 1033–1036.
- 177 B. A. Grzybowski, A. Winkleman, J. A. Wiles, Y. Brumer and G. M. Whitesides, *Nat. Mater.*, 2003, **2**, 241–245.
- 178 P. W. H. Pinkse, T. Fischer, P. Maunz and G. Rempe, *Nature*, 2000, **404**, 365–368.
- 179 G. M. Whitesides and B. Grzybowski, *Science*, 2002, **295**, 2418–2421.
- 180 B. A. Grzybowski and C. J. Campbell, *Chem. Eng. Sci.*, 2004, **59**, 1667–1676.
- 181 Z. Tabor, E. Rokita and T. Cichocki, *Phys. Rev. E: Stat. Phys., Plasmas, Fluids, Relat. Interdiscip. Top.*, 2002, **66**, 51906.
- 182 S. Dano, P. G. Sorensen and F. Hynne, *Nature*, 1999, **402**, 320–322.
- 183 V. K. Vanag, L. F. Yang, M. Dolnik, A. M. Zhabotinsky and I. R. Epstein, *Nature*, 2000, **406**, 389–391.
- 184 H. W. Horch and L. C. Katz, *Nat. Neurosci.*, 2002, **5**, 1177–1184.
- 185 J. S. Turner, J. C. Roux, W. D. McCormick and H. L. Swinney, *Phys. Lett. A*, 1981, **85**, 9–12.
- 186 J. C. Roux, R. H. Simoyi and H. L. Swinney, *Physica D*, 1983, **8**, 257–266.
- 187 S. K. Scott, *Chemical Chaos*, Oxford University Press, New York, 1991.
- 188 F. Arteaga-Larios, E. Y. Sheu and E. Perez, *Energy Fuels*, 2004, **18**, 1324–1328.
- 189 K. J. M. Bishop, M. Fialkowski and B. A. Grzybowski, *Proc. Natl. Acad. Sci.*, 2005 submitted.